SELECTED STUDIES OF UNDERWATER SOUND PHENOMENA

15 OCTOBER 1966

AVCO MARINE ELECTRONICS OFFICE

Selected Studies of Underwater Sound Phenomena

by

H. W. Marsh and R. H. Mellen
AVCO Marine Electronics Office
New London, Conn.

15 October 1966

The work summarized in this report was supported by
The Acoustics Programs, Office of Naval Research
under Contract Number Nonr 3353 (00)

MED-66-1005

Selected Studies of Underwater Sound Phenomena

Preface

This document reports on three separate studies conducted during fiscal year 1966. Pagination, references and figures are numbered separately for each study.

Part I, Some Stochastic Structures for Modeling Underwater Sound, discusses simulation of propagation, reverberation and ambient noise with an underlying stochastic description of the sea surface.

Part II, Spectra of The Dynamic Sea Surface proposes a unified model of the equilibrium sea surface, including turbulence and based on observations of several different features of the sea.

Part III, System Parameters for Ultrasonic Explosive Echo-Ranging, illustrates the significance of high frequencies (up to 40 kHz) to permit improved directional discrimination.

Some Stochastic Structures for Modeling Underwater Sound

H. W. Marsh *

Abstract

Several stochastic structures are described which may be used to model certain features of the underwater sound field. These include propagation (and reverberation) and sea noise. Emphasis is placed upon models which are adapted to digital computation, in which wave forms are of interest, in addition to averages such as power spectra.

May 20, 1966

* AVCO Marine Electronics Office, New London, Connecticut

The research reported here has been sponsored by The Acoustics Programs, U. S. Office of Naval Research and was presented at Applications of Stochastic Theory in Underwater Acoustics, University of Rhode Island (June 6, 7, 1966)

Introduction

The principal source of stochastic effects upon underwater sound is the dynamic sea surface. There are, of course, other water motions, including tides, internal waves and currents. However, these generally tend to produce rather smaller effects and of longer periods than the wind driven sea. Furthermore, in a compromise between scope and detail, our attention is going to be focused on a simple, but important, underwater sound situation in which the presence of the sea bottom and of sound velocity structure are not emphasized. We shall not treat sea noise other than that which is generated by the sea surface. Under these conditions, a single stochastic function, the turbulence spectrum of wind driven waves, is sufficient to permit modeling of noise, propagation and reverberation. We shall discuss the turbulence spectrum, and show a model of the sound field which can be expected to produce covariance (space-time) functions which are indistinguishable from measurements. More than this is obtainable from the model: wave forms. While the wave forms cannot be defended upon empirical grounds, since measurements are very limited, they will at least serve as a guide to what may be expected. Further, by following in the footsteps of Stocklin[1], the field continuum may be recovered to the extent shown by his theory of space-time sampling. The modeling will be described in a hybrid context. This permits interspersed use of actual sound recordings and digital simulation, as well as flexibility in choosing specific mechanizations. We have not yet produced an entire simulation, but will show examples of results to date.

The Physical Situation

A simple sound source is located at the origin of coordinates. At a distance R from the source, the free field pressure $f(t - R/c)/R$ is assumed, for constant sound speed c. If non-linear propagation effects can be neglected, an extended, directional source may be considered, and near field effects included without difficulty. However, in order to accommodate non-linear effects, we shall deal here with source characteristics dependent only upon the radial coordinate.

At any point in the medium, with position vector $\underline{R}$ (x, y, z) the total sound field will be

$$p(\underline{R}, t) = P_a + P_d + P_s \qquad (1)$$

P_a denotes the ambient pressure, entailing the hydrostatic head as modulated by the moving sea surface. P_d and P_s are produced by the source, and denote respectively a direct arrival and an arrival scattered by the sea surface. P_s in turn will consist of a coherent component P_{coh}, corresponding to ordinary reflection with inversion of sign and loss of amplitude, and an incoherent component P_{inc}. The latter is "reverberation".

The sea surface lies at a mean elevation Z_0 above the sound source and is described by the instantaneous elevation $Z(x, y, t)$. Its form and motion determines the ambient pressure and scattered component of the sound field.

The Dynamic Sea Surface

The representation (and justification therefor) which we shall employ

has been discussed by Marsh[2] et al. Briefly, we have the isotropic turbulence spectrum H (K, ω). The auto covariance function of surface elevation is ρ:

$$\rho(r,\tau) = \langle Z(x,y,t)\, Z(x+\xi,\ y+\eta,\ t+\tau)\rangle \qquad (2)$$

where <> represents an ensemble average and $r^2 = \xi^2 + \eta^2$. The turbulence spectrum is defined to be

$$H(K,\omega) = \frac{K}{2\pi^2}\int_0^\infty\int_0^\infty \rho(r,\tau)\cos(\omega\tau)J_0(Kr)\,r\,dr\,d\tau \qquad (3)$$

This is the ordinary three dimensional power spectrum; the Bessel function J_0 enters because of assumed isotropy. There are also the marginal spectra

$$A^2(K) = \int_0^\infty H(K,\omega)\,d\omega \text{ and } B^2(\omega) = \int_0^\infty H(K,\omega)\,dK. \qquad (4)$$

If K and ω are functionally related, we have $A^2(K)\,dK = B^2(\omega)\,d\omega$, and then H (K, ω) has values only on the diagonal $K = K(\omega)$. In this case we speak of dispersion, and there is a definite speed $v = \omega/K(\omega)$ for each wave number. The classical dispersion relation

$$\omega^2 = gK + \gamma K^3 \qquad (5)$$

(g = acceleration of gravity and γ the specific surface tension, about 74 cgs for clear water) defines a minimum phase velocity $v = (4\gamma g)^{1/4}$, which corresponds to a wave frequency near 14 Hz and wave length of about 2 cm. Waves longer than this are gravity controlled and dispersive:

$$\begin{aligned} A^2(K) &= \beta \exp(-2v^2/S^2)/2K^3 \\ B^2(\omega) &= \beta\, g^2 \exp(-2v^2/S^2)/\omega^5 \end{aligned} \qquad (6)$$

for a wind speed S. The dimensionless constant β is 7.4×10^{-3}.

Short waves are turbulent, and

$$H(K, \omega) = \exp(-v^2 / 2 v_{00}^2) \beta \sqrt{\pi/2}^1 / K^4 v_{00} \qquad (7)$$

where $v = \omega/K$, $v_{00} = v_0 (K_0/K)^{1/4} N$, and the numeric N is

$$\left[3 \sqrt{2\pi}/4^2 \; 2^{5/6} \Gamma(11/6)\right]^{3/8}$$

The transition region near the minimum phase velocity, is unfortunately not well defined, although there is evidence that turbulence extends somewhat into the gravity range.

Ambient Pressure

Marsh[3] has shown that the power spectrum of surface generated noise is proportional to the sea surface velocity spectrum which is simply $\omega^2 B^2(\omega)$. In like manner, the cross spectra of pressures at separated points may be obtained from a weighted integral of the turbulence spectrum, with weight dependent upon the geometry. We are not yet able to report results on these cross spectra, but will use measured or postulated covariance functions which are consistent with the desired power spectra. Such covariance functions are reported in the literature by Cron[4], and others. Modeling wave forms with prescribed cross spectra will be taken up below.

Propagation

The direct arrival has been described by Marsh et al[5]. The controlling equation is

$$(q + \partial/\partial\tau)y_\xi = (q + \partial/\partial\tau)(yy_\tau) + (q\zeta_1 y_{\tau\tau} + \zeta_2 y_{\tau\tau\tau})\exp\xi \qquad (8)$$

y is the scaled pressure:

$$y = 2Bp R/p_0$$

ξ the scaled range:

$$\xi = \ln(R/R_0)$$

the local time:

$$\tau = t - R/c_0$$

q, ζ_1 and ζ_2 are relaxation and viscous coefficients characteristic of sea water; B is determined by the lowest order non-linear terms in the equation of state, and p_0 is a reference pressure. Integration of the equation from a prescribed wave form f(t) at reference range R_0 has been described. The same equation may be used to determine the coherent scattered wave if R is taken to be the total path length, if the sign of y is reversed, and the amplitude reduced by a factor 1 - a. Measurements and theory for this "surface loss" have been reported[6]. The flux which is lost from the coherent wave reappears in the incoherent wave, distributed in angle and frequency. The incoherent power spectrum at a point may be obtained from a weighted integral of the surface turbulence spectrum, with weight dependent upon geometry, and in a similar manner, the cross spectra at separated points

may be obtained. Here again, we have no results to quote on cross spectra. Two simple cases have been investigated, as follows. For monostatic reverberation, the power spectrum of the reverberation is

$$S_R(\omega) = M(t) \int_{-\infty}^{\infty} \omega_0^3 \left| E(\omega_0) \right|^2 H(K, \omega - \omega_0) d\omega_0 \qquad (9)$$

$$M(t) = 128 R_0^2 Z_0^4 / c^9 \cos\theta \, t^7$$

$$K = 2\omega_0 \cos\theta / c \; ; \; \sin\theta = 2Z_0 / ct$$

Actually, since the factor M depends upon time, this is a pseudo-spectrum. Its nature and some of its limitations are discussed by Faure[7]. The quantity $E(\omega)^2$ is the "energy" spectrum of the pressure form f(t):

$$E(\omega)^2 = \left| \int_{-\infty}^{\infty} f(t) \exp(i\omega t) dt \right|^2 \qquad (10)$$

For short signals with energy scattered mainly by gravity waves, the pseudo-power-spectrum of the monostatic reverberation is proportional to the signal "energy" spectrum.

The other example concerns forward scatter. For frequencies below a few kHz, depending upon geometry and sea conditions, the incoherent component of the field will consist of upper and lower side bands of spectrum proportional to the marginal surface frequency spectrum[8]. For an isotropic sea the side bands will be equal in intensity, but not if the sea is directional. The percent modulation is, as indicated previously, determined by the "surface loss" in such a way that the total flux of energy incident upon the surface is recovered in the scattered field.

Simulation

In the sequel, we shall discuss simulation without regard to the particular stochastic elements involved. This will permit us to update knowledge of sea noise, propagation, etc. and to introduce "real" data at will. Although the simulation will be electrical, we shall maintain sound pressure units throughout. We deal with an array of pressures $p_n(t)$ and sampled equivalents

$$\hat{p}_{nm} = p_n(mT) \tag{11}$$

which are quantized and obtained with the sampling interval T. In our simulation to date we have used 12 bit quantization and intervals as small as one microsecond. By way of notation, the hat (circumflex) will show that the quantities is a sample value of a continuous variable. On the other hand, a number derived (e. g., by filtering) from p_{nm} will not carry the hat. If only a single pressure function is of interest, the first subscript will not be written.

Filtering, or spectral modification of p (t) may be simulated by a transversal digital filter[9]. The relation

$$y_m = \Sigma A_n \hat{p}_{m-n} + \Sigma B_n y_{m-n} \tag{12}$$

corresponds to filtering with a rational function frequency response. The coefficients A_n, B_n are determined by the filter poles and zeros. A simple low pass filter requires 2 coefficients; a high pass, 3 and a band pass 4.

Phase Shifter

The frequency response $(\lambda + i\omega)/(\lambda - i\omega)$ is all pass, with phase ranging from zero at low frequency to π at high. A corresponding digital filter relation is

$$(1 + x)y_m = (1 - x)\hat{p}_m + x\hat{p}_{m-1} + xy_{m-1} \qquad (13)$$

By cascading, and series parallel arrangements of several basic phase shifters, any desired phase shift frequency characteristic can be approximated, and then multi channel wave forms with prescribed cross spectra can be simulated.

Random Number Generator

Simulation of a stochastic variable starts with a random number sequence. The scheme we have used is described in the literature[10, 11]. Let R_n be a random number, and $(R_n)_S$ the operation of shifting the number in binary form a given number of (binary) digits to the left. Then if K is a constant, and

$$R_n = (KR_{n-1})_S, \qquad (14)$$

some K numbers may be generated before repetition. The first number should be odd; otherwise zero might develop, with early termination of the sequence. It is stated that K should be a large odd power of five. Our Recomp III uses a 40 bit word. $K = 5^{17}$ is a satisfactory choice, with left shift of 12 bits and retention of 28 bits. Other choices of K and shift have been inferior in one respect or another. Starting with $R_0 = 2^{15} + 1$, and

scaling $|R_n| \leq 1$, $R_1 = -0.4700$. Table I then gives the distribution of amplitudes and zero crossing intervals of the first 10,000 numbers. It may be seen that the sequence is nearly uniformly distributed between -1 and +1, and the intervals between zero crossings approximate the desired distribution $P_n = 2^{-n-1}$. A chi-square test on the tables gives a confidence level of 95% for the desired distributions.

Simulation of Sea Noise

A simple choice is "pink" noise, P_m for which we use a low pass filter:

$$P_m = cR_m + xP_{m-1} \tag{15}$$

Assuming the R_m to have the auto covariance

$$\langle R_m R_n \rangle = \sigma^2 \delta_{mn} = \sigma^2, \; m-n$$
$$= 0, \; m \neq n,$$

the P_m have the auto covariance

$$\langle P_m P_n \rangle = \frac{c^2 \sigma^2 x}{1 - x^2}^{|m-n|} \tag{16}$$

For the noise reported here, $\sigma^2 = 1/3$. We have used $x = 0.995$, $c = 0.005$, which corresponds to a power spectrum down 3dB from its low frequency maximum at about 800 Hz, for a sampling interval of 1μ sec. Table II gives the distribution of amplitudes and zero crossing intervals of the first 10,000 P_m. The maximum value of P_m in this interval was 0.095, there being 7 negative and 5 positive values close to this number.

A more elaborate, and a realistic representation of sea noise requires the simulation of surface waves. with amplitude spectrum $B^2(\omega)$. To date, we have preapred a simulation covering the gravity region, and one in the short capillary region. For the first, we use Equation (6).

$$e^{-a/x} \approx \left(\frac{Nx}{a+Nx}\right)^N$$

for large N. The term ω^{-5} can be approximated by low and high pass filters. Figure 1 gives an example, with formulae, using N = 40, for a total of 48 coefficients in the equivalent transversal filter. In the capillary region, Equation (7) leads to

$$B^2(\omega) \sim \omega^{-11/3} \qquad (17)$$

This can be approximated by six coefficients as shown in Figure 2.

Simulation of Reverberation

If the approximations leading to Equation (9) and discussed following Equation (10) are accepted, the reverberation spectrum (pseudo) is proportional to the signal energy spectrum. For an explosive source, the energy spectrum of the main part of the wave of detonation is proportional to $1/(4\pi^2 f_0^2 + \omega^2)$. The cutoff frequency f_0 is determined by the explosive yield, hydrostatic pressure and, to a small extent, range, and typically is the order of one kHz for yields of a few pounds. Thus, the pink noise discussed above is also a simulation for reverberation. Figure 3 displays the wave from short portions of a reverberation record of 3.8# of TNT, sampled at a rate of 40 kHz. Figure 4 gives the distribution of amplitudes of 2000 sample points, and also the distribution of pink noise with f_0 = 800 Hz and the same sampling rate. The amplitude distributions are similar, and the

zero crossings are fairly alike, as may better be seen in Figure 5, which shows the probability distributions of the samples. The amplitude distribution of the noise is easily tailored by adding together a few independent random numbers. The law of large numbers works rapidly, and 10 or so numbers added together provide an excellent normal distribution.

Summary

We have sketched here a method of similating underwater sound, emphasizing the influence of the dynamic sea surface and the use of digital wave form synthesis. Although the methodology and results presented represent hardly more than a beginning, it is believed that known properties of real sounds can be accurately simulated. Modern computers are so fast that real time simulation is now a reality, and it is inevitable that digital filtering will be of increasing value for on-line processing.

Table I. Distributions of 10,000 Random Numbers ($K=5^{17}$)

Amplitudes

- 1.0	To	- 0.9	470
- 0.9	To	- 0.8	517
- 0.8	To	- 0.7	498
- 0.7	To	- 0.6	508
- 0.6	To	- 0.5	517
- 0.5	To	- 0.4	481
- 0.4	To	- 0.3	515
- 0.3	To	- 0.2	506
- 0.2	To	- 0.1	511
- 0.1	To	- 0.0	494
- 0.0	To	0.1	493
0.1	To	0.2	493
0.2	To	0.3	540
0.3	To	0.4	489
0.4	To	0.5	513
0.5	To	0.6	498
0.6	To	0.7	506
0.7	To	0.8	494
0.8	To	0.9	467
0.9	To	1.0	490

Zero Crossing Intervals

Interval	Positive	Negative
1	1273	1235
2	625	690
3	328	300
4	150	167
5	97	68
6	31	33
7	15	17
8	4	10
9	4	6
10	2	2
11	0	1
12	1	1
13 and more	0	0

Table II **Distributions of 10, 000 values of Pink Noise ($K=5^{15}$)**

Amplitude			Number
- 0. 10	To	0. 09	7
- 0. 09	To	0. 08	39
- 0. 08	To	0. 07	189
- 0. 07	To	0. 06	248
- 0. 06	To	0. 05	477
- 0. 05	To	0. 04	756
- 0. 04	To	0. 03	819
- 0. 03	To	0. 02	880
- 0. 02	To	0. 01	998
- 0. 01	To	0. 00	1324
0. 00	To	0. 01	1263
0. 01	To	0. 02	981
0. 02	To	0. 03	598
0. 03	To	0. 04	505
0. 04	To	0. 05	289
0. 05	To	0. 06	326
0. 06	To	0. 07	193
0. 07	To	0. 08	83
0. 08	To	0. 09	20
0. 09	To	0. 10	5

Zero Crossing Interval

No.	Positive	Negative
1	54	65
2	22	17
3	13	13
4	12	9
5	6	4
6	5	5
7	2	2
8	3	2
9	4	2
10	1	4
11	1	2
12	0	0
13	1	0
14	2	3
15	2	1
16	1	0
17	5	4
18	1	1
19	3	0
20	0	3

Zero Crossing Interval

No.	Positive	Negative
21	3	0
22	1	0
23	1	0
24	1	1
25	1	2
26	1	1
27	0	0
28	0	0
29	0	0
30	0	1
> 30	47	
largest interval	1138	

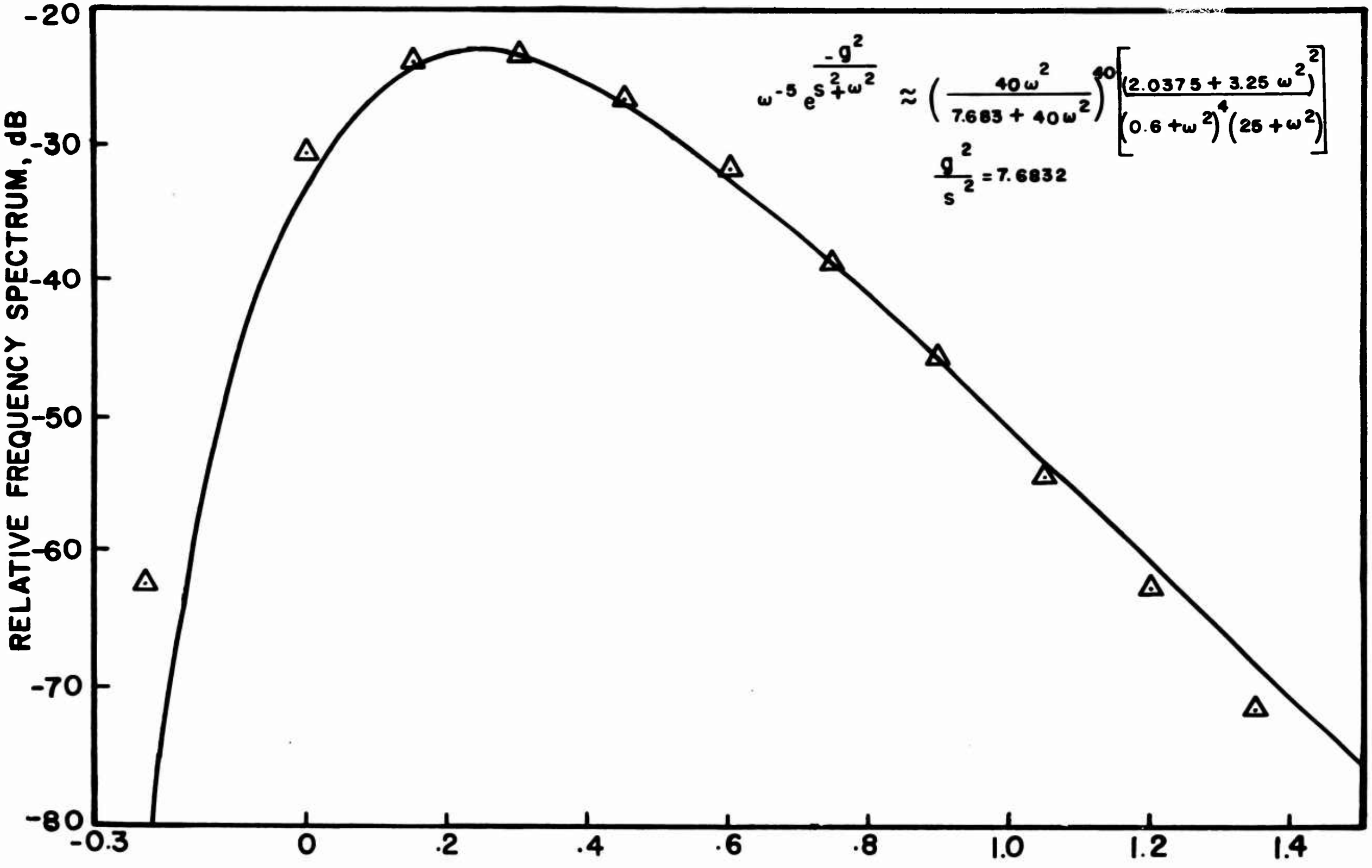

1. APPROXIMATION TO GRAVITY WAVE SPECTRUM.
LINE IS DESIRED FORM; POINTS ARE FROM APPROXIMATING FORMULA.

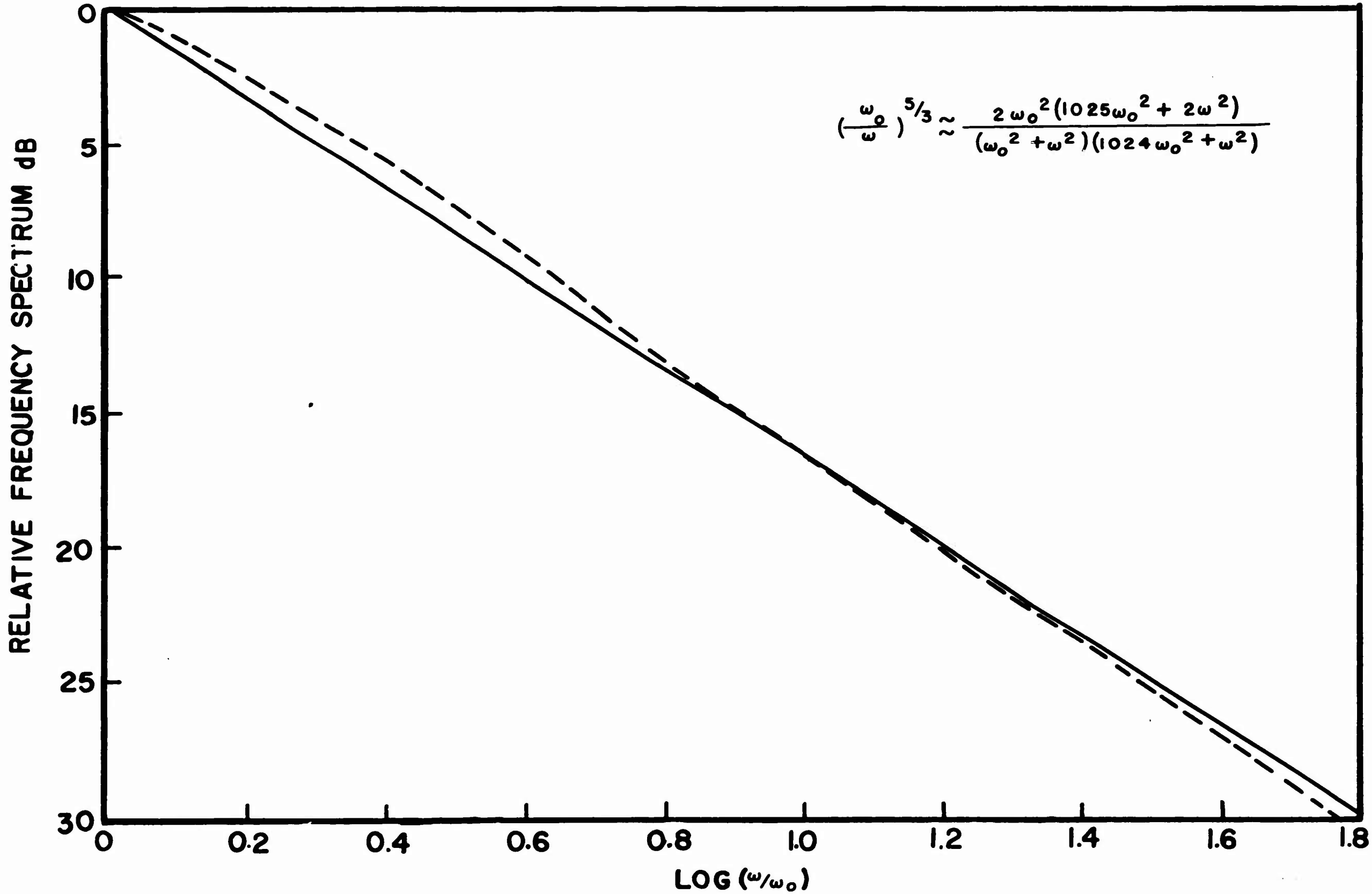

2. APPROXIMATION TO CAPILLARY WAVE SPECTRUM.
LINE IS DESIRED FORM; POINTS ARE FROM APPROXIMATING FORMULA

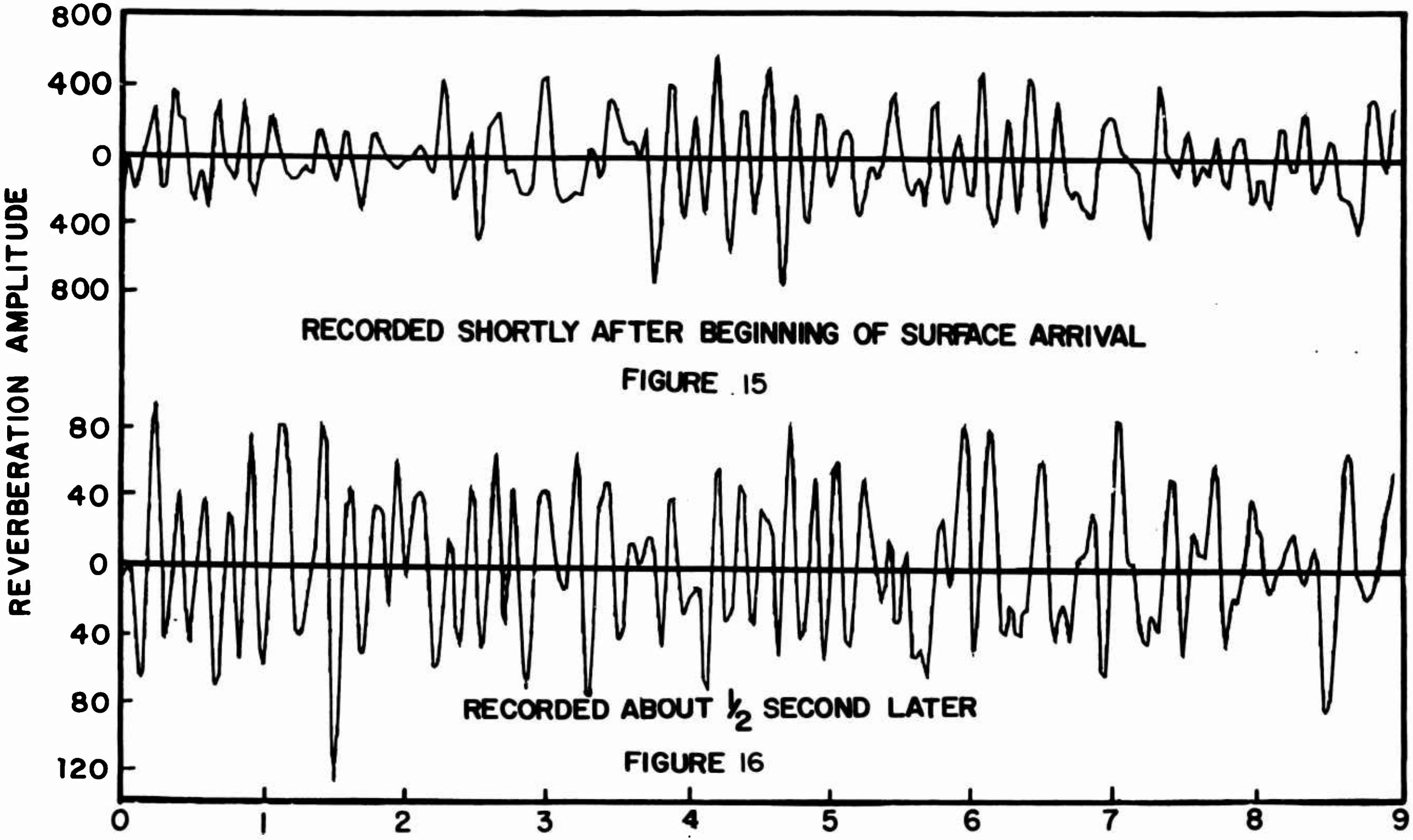

3. WAVE FORM OF 12.5 ms OF SURFACE REVERBERATION FROM 3.8 POUNDS OF TNT. SAMPLES WERE TAKEN SHORTLY AFTER THE BEGINNING OF THE SURFACE RETURN (TOP TRACE) AND SOMEWHAT LATER, WELL DOWN ON THE DECAY CURVE (BOTTOM TRACE).

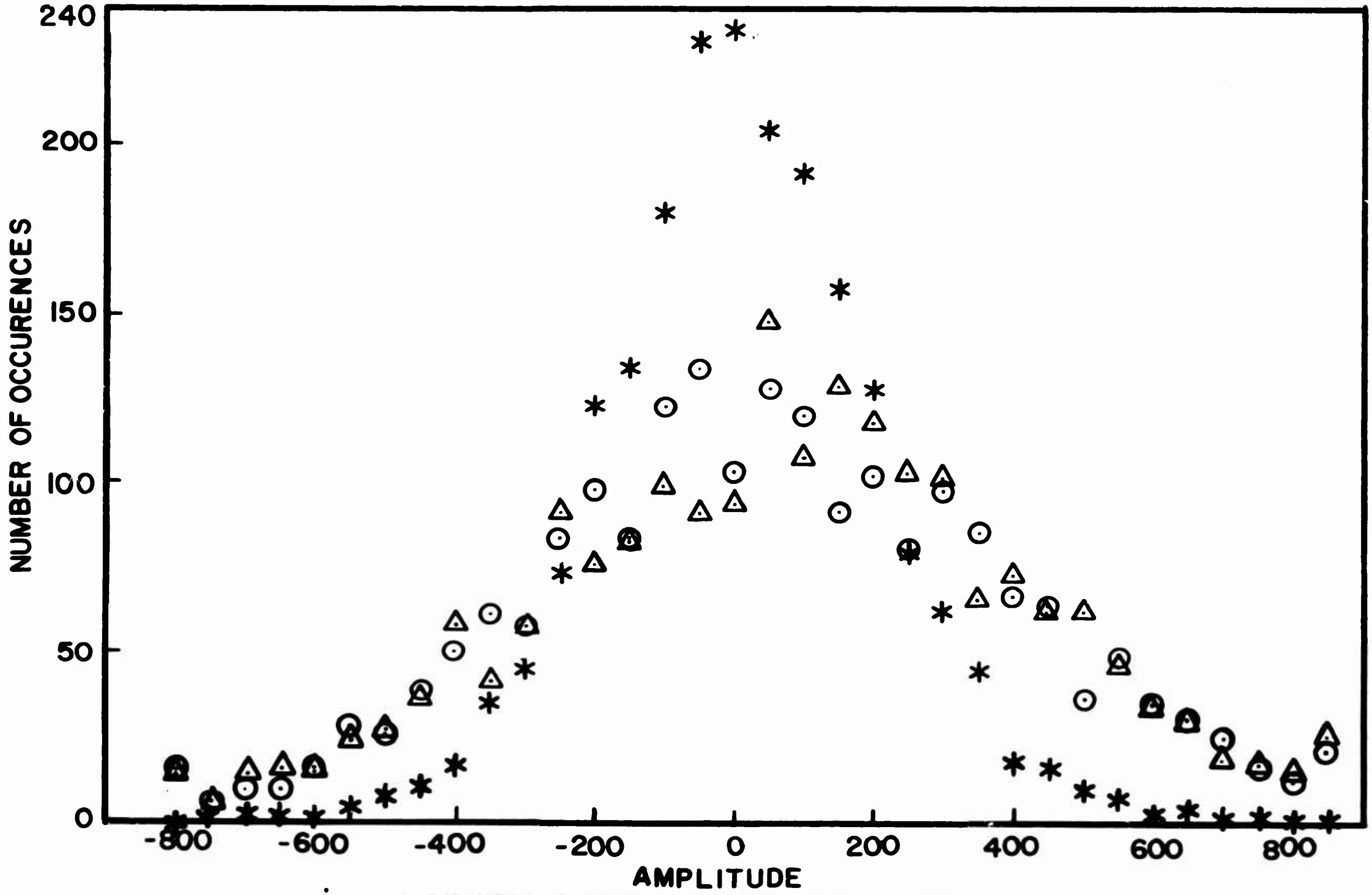

4. DISTRIBUTIONS OF AMPLITUDES OF REVERBERATION AND PINK NOISE. AMPLITUDE SCALE FOR "LATE" REVERBERATION IS TEN TIMES THAT OF EARLY REVERBERATION AND PINK NOISE.

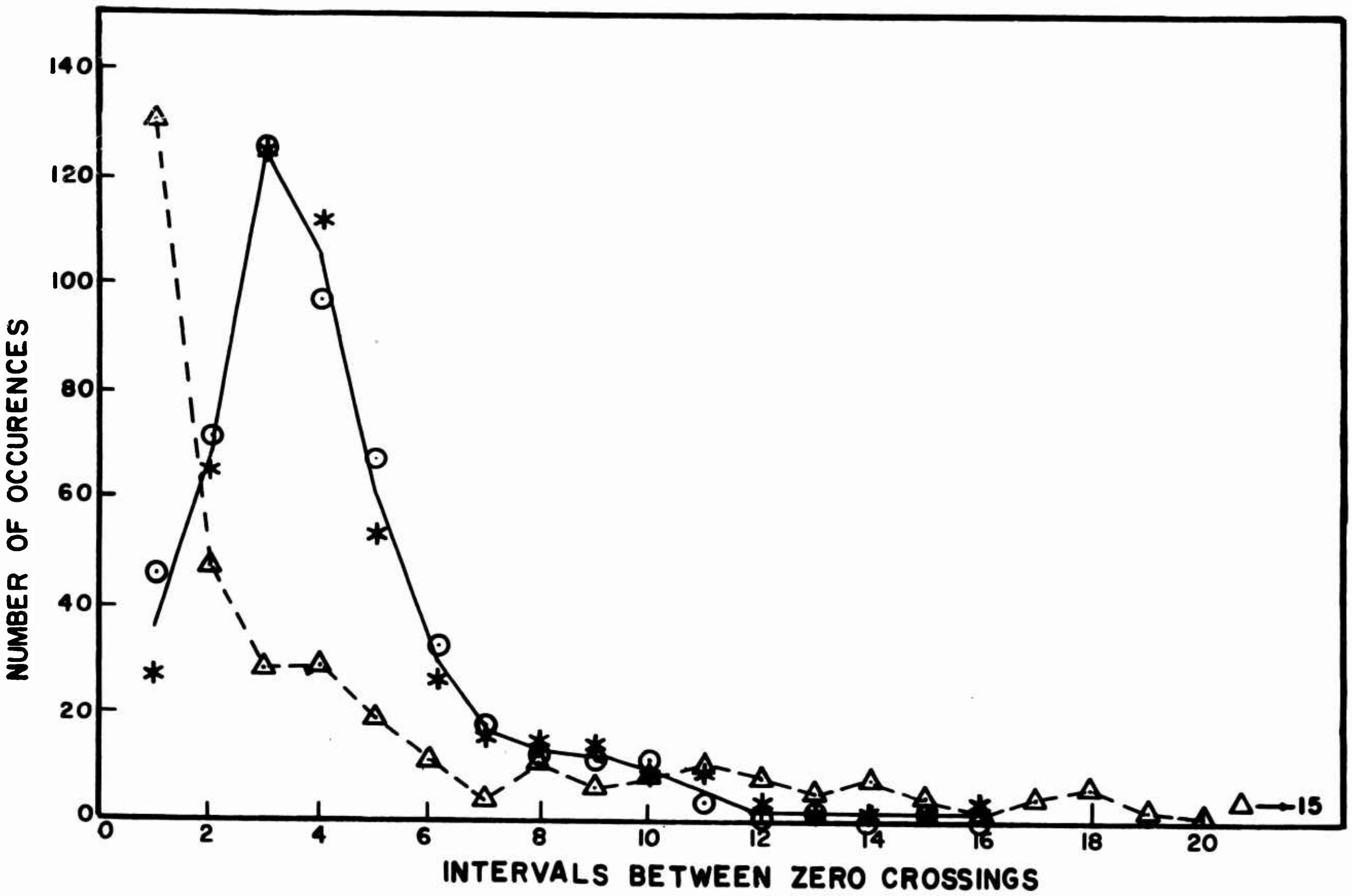

5. DISTRIBUTION OF ZERO CROSSINGS OF REVERBERATION AND PINK NOISE.

References

1. P. L. Stocklin, Doctoral Dissertation,
University of Connecticut (1961).

2. H. W. Marsh and R. H. Mellen,
Spectra of The Dynamic Sea Surface, (Unpublished manuscript),
AVCO Corporation, New London, Conn. (October 1965).

3. H. W. Marsh,
Origin of The Knudsen Spectra,
J. Acoust. Soc. Am. 35, 409-410 (March 1963).
See also E. Y. T. Kuo, Doctoral Dissertation, University of Conn. (1966).

4. B. F. Cron and C. H. Sherman,
Spatial-Correlation Functions for Various Noise Models,
J. Acoust. Soc. Am. 34, 1732-1736 (1962); 38, 885 (L) (1965).

5. H. W. Marsh et al;
Anomalous Absorption of Pressure Waves from Explosions in Sea Water;
J. Acoust. Soc. Am. 38, 326 (August 1965);
Propagation and Reception of Transient Underwater Sounds,
AVCO Marine Electronics Office, 15 September 1966

6. H. W. Marsh et al;
Scattering of Underwater Sound by The Sea Surface,
J. Acoust. Soc. Am. 33, 334-340 (March 1961);
Sound Reflection and Scattering by The Sea Surface,
J. Acoust. Soc. Am. 35, 240-244 (February 1963)

7. P. Faure,
Theoretical Model of Reverberation Noise,
J. Acoust. Soc. Am. 36, 259-266 (February 1964)

8. H. W. Marsh and E. Y. T. Kuo,
Further Results on Sound Scattering by The Sea Surface
(Unpublished manuscript),
AVCO Corporation, New London, Conn. (October 1965).

9. R. B. Blackman,
Data Smoothing and Prediction,
Addison-Wesley Publishing Co., Reading, Mass. (1965).

10. H. Kahn,
Multiple Quadrature by Monte Carlo Methods, in Mathematical Methods for Digital Computers,
A. Ralston and H. S. Wilf (eds.),
John Wiley and Sons, Inc., New York (1962).

11. H. A. Meyer (ed.),
Symposium on Monte Carlo Methods,
John Wiley and Sons, Inc., New York (1956).

Figures

1. Approximation to Gravity Wave Spectrum.
   Line is desired form; points are from approximating formula.

2. Approximation to Capillary Wave Spectrum.
   Line is desired form; points are from approximating formula.

3. Wave form of 12.5 ms of surface reverberation from 3.8 pounds of TNT. Samples were taken shortly after the beginning of the surface return (top trace) and somewhat later, well down on the decay curve (bottom trace).

4. Distributions of amplitudes of reverberation and pink noise. Amplitude scale for "late" reverberation is ten times that of early reverberation and pink noise.

5. Distribution of zero crossings of reverberation and pink noise.

Spectra of The Dynamic Sea Surface

H. W. Marsh* and R. H. Mellen*

Abstract

A unified model of the equilibrium surface, including turbulence, is proposed. The model is based upon interpretations of a variety of measurements, including physical (wave staff); optical glitter and slope; radar and sonar scatter and acoustic ambient noise.

October 1, 1965

*AVCO Marine Electronics Office, New London, Conn.
This study was supported by The Acoustics Programs, Office of Naval Research under Contract Nonr 3353(00).

SPECTRA OF THE DYNAMIC SEA SURFACE

Introduction

Experimental measurements of the statistical behavior of the wind-driven sea surface have proven surprisingly difficult to reconcile to a unified model. A list of some of the various methods and sources is given in Table I.

TABLE I

Category	Type of Measurement	Source
Physical	Wave height vs frequency by wave staff measurements, etc.	Burling (1955) Neumann (1953) Pierson (1955)
Optical	Slope/angle distribution by surface glitter photography	Cox (1956)
Optical	Slope spectrum vs frequency measurements by refraction of light	Cox (1958)
Radio	Radar scatter strength vs wavelength and angle, Doppler Frequency spectra	Kerr (1951) MacDonald (1962) Wiltsie (1957)
Underwater Sound	Sonar scatter strength, Doppler spectra, ambient noise spectra	Marsh (1963a, b) Marsh (1964) Mellen (1964)
Sound in Air	Scatter strength, Doppler spectra	Liebermann (1963)

The main difficulty is that each case requires appropriate theoretical interpretation. Thus, electromagnetic and acoustic scattering at "finite" wavelengths, optical refraction and reflection, ambient noise, and Doppler theories are all involved in relating these data to the dynamics of the surface. We now believe that Marsh's (1961) first order scattering theory, the surface noise radiation theory (Marsh 1963a) and Kuo's (1965) hydrodynamic theory of the turbulent surface, together with the others, give a reasonably complete picture.

According to Kuo, both turbulent surface flow and wave motion are expected to grow under the influence of the turbulent wind. The equilibrium excitation levels are known only by experiment since the theory does not consider the saturated state. We find by sonar and radar scattering measurements that the height spectrum is asymptotic to K^{-3}, independent of wind speed (figure 1)*. This gives a scattering strength that is also independent of wavelength (figure 2)*.

From Doppler measurements at short wavelengths (figure 3)*, we also find that the associated frequency or horizontal velocity spectra are not related to the wavenumber spectrum by the gravity-surface tension dispersion formula. Instead, the surface appears to act more like a turbulent boundary layer. At very long wavelengths, however, radio measurements do show Doppler frequencies associated with the resonant gravity wavelengths. Also, from forward scatter Doppler calculations (figure 4)*, we find a similar situation since the Doppler spectrum is dominated by the longest wavelengths, and, indeed, is the weighted surface frequency spectrum.

---

*See figures and discussion and conclusion below.

In the gravity region according to surface wave theory, the K^{-3} wavenumber spectrum transforms to the ω^{-5} frequency spectrum, which agrees with results obtained directly from wave height measurements. In the capillary region, however, the experimental results do not agree with wave theory. The frequency spectrum is derived from both Doppler and ambient noise measurements and gives $\omega^{-11/3}$ instead of $\omega^{-7/3}$.

The transition between gravity waves and turbulent flow is not known with any exactness. In fact, the surface may be truly wavelike only for the longest existing wavelengths. Complete turbulence may be estimated to begin somewhere near the group velocity minimum for which $K = 202 m^{-1}$. However, the transition appears to involve most of the gravity spectrum.

It does not appear likely that specific surface details such as breaking waves, spume, etc., will alter the picture because all these appear to be included in the statistical description of the random dynamic surface.

Theory

Observations and analyses drawn from a number of sources have been interpreted to provide an estimate of the wave number and frequency spectra of the wind driven sea elevation. A brief summary is given here, covering frequencies up to 5×10^4 Hz and wave numbers to $10^4 m^{-1}$. The results are given for a fully developed sea, in equilibrium with the local wind, in terms of an equivalent isotropic spectrum.

The xy plane corresponds to the mean surface. The instantaneous elevation $z = \zeta(x, y, t)$ has the auto covariance $\rho = < \zeta(x, y, t)\, \zeta(x+\xi, y+\eta, t+\tau) >$. A stationary, homogeneous, isotropic statistical surface is postulated, and then ρ depends only upon τ and $r = (\xi^2 + \eta^2)^{1/2}$. A convenient two dimensional spectrum is

$$H(K, \omega) = \frac{K}{2\pi^2} \int_0^\infty \int_0^\infty \rho(r, \tau) \cos \omega\tau \; J_0(Kr)\, r\, dr\, d\tau$$

which has the inverse relationship

$$\rho(r, \tau) = \int_0^\infty \int_0^\infty H(K, \omega) \cos \omega\tau \; J_0(Kr)\, dK\, d\omega$$

Thus, the variance (mean square wave height), $h^2 = \rho(o, o)$, is distributed over the spectrum $H(K, \omega)$; there are the marginal spectra

$$A^2(K) = \int_0^\infty H(K, \omega)\, d\omega = \frac{K}{2\pi} \int_0^\infty \rho(r, o)\, J_0(Kr)\, r\, dr$$

and

$$B^2(\omega) = \int_0^\infty H(K, \omega)\, dK = \frac{1}{\pi} \int_0^\infty \rho(o, \tau) \cos \omega\tau \; d\tau \, .$$

The variance is given in terms of either of the marginal spectra:

$$h^2 = \int_0^\infty A^2(K)\,dK = \int_0^\infty B^2(\omega)\,d\omega .$$

There is the dispersion equation for surface waves in deep water (neglecting viscosity) which relates ω and K:

$$\omega^2 = gK + \gamma K^3$$

Here, g is the acceleration of gravity and γ the specific surface tension (about 74 cgs for clean water). When the dispersion relationship applies, $H(K, \omega)$ is relevant only on the diagonal corresponding to $K = K_0(\omega)$

$$H(K, \omega) = A^2(K)\,\delta(K - K_0) = B^2(\omega)\,\frac{d\omega}{dK_0}\,\delta(K - K_0) .$$

K_0 satisfies the dispersion equation and δ is the Dirac function. In any event, the relation

$$\frac{d\omega}{dK} = \frac{A^2(K)}{B^2(\omega)}$$

defines a functional relationship between K and ω, which we may call the mean dispersion. If $H(K, \omega)$ is not diagonal, the surface elevation is turbulent instead of wavelike. In this case, there is no deterministic dispersion equation, but only mean dispersion.

For dispersive waves, the phase velocity is $v = \omega/K = (g/K + \gamma K)^{1/2}$. The minimum velocity $v_0 = (4\gamma g)^{1/4}$, corresponding to $K_0 = (g/\gamma)^{1/2}$ and $\omega_0 = (4g^3/\gamma)^{1/4}$. Waves for which $K < K_0$ are the gravity waves; those for which $K > K_0$ are the capillary waves.

The Spectra

I. Gravity region: In the gravity region, dispersive waves predominate. The spectra are of the form

$$A^2(K) = \beta \exp(-2v^2/s^2)/2K^3$$

$$B^2(\omega) = \beta g^2 \exp(-2v^2/s^2)/\omega^5$$

for a wind speed s. The dimensionless constant β is 7.4×10^{-3}, according to Burling (1955). These spectra are in general agreement with the results of Pierson (1964).

II. Capillary region: In the capillary region, turbulence predominates. The marginal spectra are found to be

$$A^2(K) = \beta/2K^3$$

$$B^2(\omega) = \beta g^2/\omega_0^{4/3}\,\omega^{11/3}$$

Note that the Burling spectrum persists; the frequency spectrum has changed form in accordance with the shift from gravity to surface tension control. The entire spectrum $H(K, \omega)$ is displayed in cross section in Figure 2, (see discussion and conclusions below). These may be approximated by the formula

$$H(K,\omega) = \exp(-v^2/2v^2_{00})\ \beta/\sqrt{\pi/2}\ K^4 v_{00}$$

where $v = \omega/K$ and $v_{00} = v_0 (K_0/K)^{1/4} N$. The numeric N is equal to

$$\left[3\sqrt{2\pi}/16\ (2)^{5/6}\ \Gamma(11/6)\right]^{3/8}.$$

Discussion and Conclusions

Figure 1 is an idealized height-wavelength spectrum for two wind speeds, 5 and 10 ms^{-1}, illustrating the asymptotic K^{-3} dependence in the saturated region and wind speed dependence of cutoff.

Sonar and radar measurements of the sea surface backscatter appear to show independence of wavelength and the predicted angular dependence of scattering strength consistent with the asymptotic K^{-3} height spectrum. Figure 2 illustrates the wavelength independence as well as the angular dependence of scattering strength for a rather wide range of wavelengths.

The Doppler spectra for several wavelengths reported by various investigators are summarized in Table II. In Figure 3, the data are referred to the equivalent surface wavenumber K and the frequencies $\Delta\omega$ are referred to the apparent horizontal surface velocity by $V = \Delta\omega/K$. The normalized Doppler spectra are shown in dB relative to the maximum which is 10 dB above the baseline. Where two spectra are shown symmetrically about zero velocity (B, C, E, F, I, J, K), the original data did not distinguish the sidebands. The normalizing procedure is based on the work of Liebermann (1963) and Marsh (1963 b), using first order resonance theory. The dotted curves are $\pm V$, the classical dispersion relation. Actual spectral distributions would be governed by the radiation beam pattern. The lack of agreement between the experimental data (A, C, D, E, F, G, H) and classical theory is believed due to surface turbulence.

In Figure 4 is shown the predicted forward scatter Doppler spectrum compared with the actual surface frequency spectrum. The similarity is obvious and consistent with other forward scatter Doppler measurements.

TABLE 2

*	Reference	Type of Radiation	Frequency (kHz)	Grazing Angle	Surface Condition
A, D	Mellen (1964)	Underwater Sound	1400, 85	45	Thames River
B	Liebermann (1963)	Sound in Air	78	70, 56 [+]	Waves in tank
C, E	Kerr (1951) [**]	Radar	3, 3, 24 ($\times 10^6$)	~ 0	at sea
F	Mason	Underwater Sound	7.5	< 45	at sea
G	Schumacher	Underwater Sound	4.0	~ 0	at sea
H	Pederson	Underwater Sound	0.7	~ 0	at sea
I, J, K	MacDonald (1963)	Radar	13, 18, 24 ($\times 10^3$)	~ 0	at sea

* Letters refer to Figure 10

\+ Angles of the incident and scattered waves

** Additional data at comparable wavelengths is reported by Wiltse [1957].

References

Burling, R W (1955), Wind generation of waves on water, Doctoral dissertation, Imperial College, University of London.

Cox, C. S. (1958), Measurements of slopes of high frequency wind wave J. Mar. Res. 16, 199-225

Cox, C S. and W. Munk (1956), Slopes of the sea surface deduced from photography of sun glitter, Bull Scripps Inst. Oceanography 6, 401.

Kerr, D. E. (1951), Propagation of Short Radar Waves, p. 580-581, (McGraw-Hill Book Co., Inc., New York, N. Y.).

Kuo, E. Y. T. (1965), On the generation of surface roughness by turbulent wind (Unpublished).

Liebermann, L. N. (1963), Analysis of rough surfaces by scattering, J. Acoust. Soc. Am. 35, 932.

MacDonald, F. G. (1963), Radar Sea Return and Ocean Wave Spectra, p. 323-329, (Prentice-Hall Inc., Englewood Cliffs, N. J.).

Marsh, H. W. (1961), Exact solution of wave scattering by irregular surfaces, J. Acoust. Soc. Am. 33, 330-333.

Marsh, H W. (1963a), The origin of the Knudsen Spectra, J. Acoust. Soc. Am. 35, 409.

Marsh, H W. (1963b), Doppler of surface reverberation, J. Acoust. Soc. Am. 35, 1836.

Marsh, H. W. (1964), Sea surface statistics deduced from underwater sound measurements, Ann. N. Y. Acad. Sci. 118, 135-146.

Mason, S. (1965) (Unpublished).

Mellen, R. H. (1964), Doppler shift of sonar backscatter from the sea surface, J. Acoust. Soc. Am. 36, 1395.

Neumann, G. (1953), On ocean wave spectra and a new method of forecasting wind-generated sea, U. S. Erosion Board, Tech. Memo, No. 43.

References (cont'd)

Pederson, M. A. (1963) (Unpublished).

Pierson, W. J., G. Neumann, and R. W. James (1955) Observing and forecasting ocean waves, U. S. Navy Hydrographic Office Publication No. 603.

Schumacher, W. E. (1964) (Unpublished).

Wiltsie, J. C., S. P. Schlesinger and C. M. Johnson (1957), Backscattering characteristics of the sea in the region from 10 to 50 KMC, Proc. IRE 45, 220-228.

List of Illustrations

Figure No.

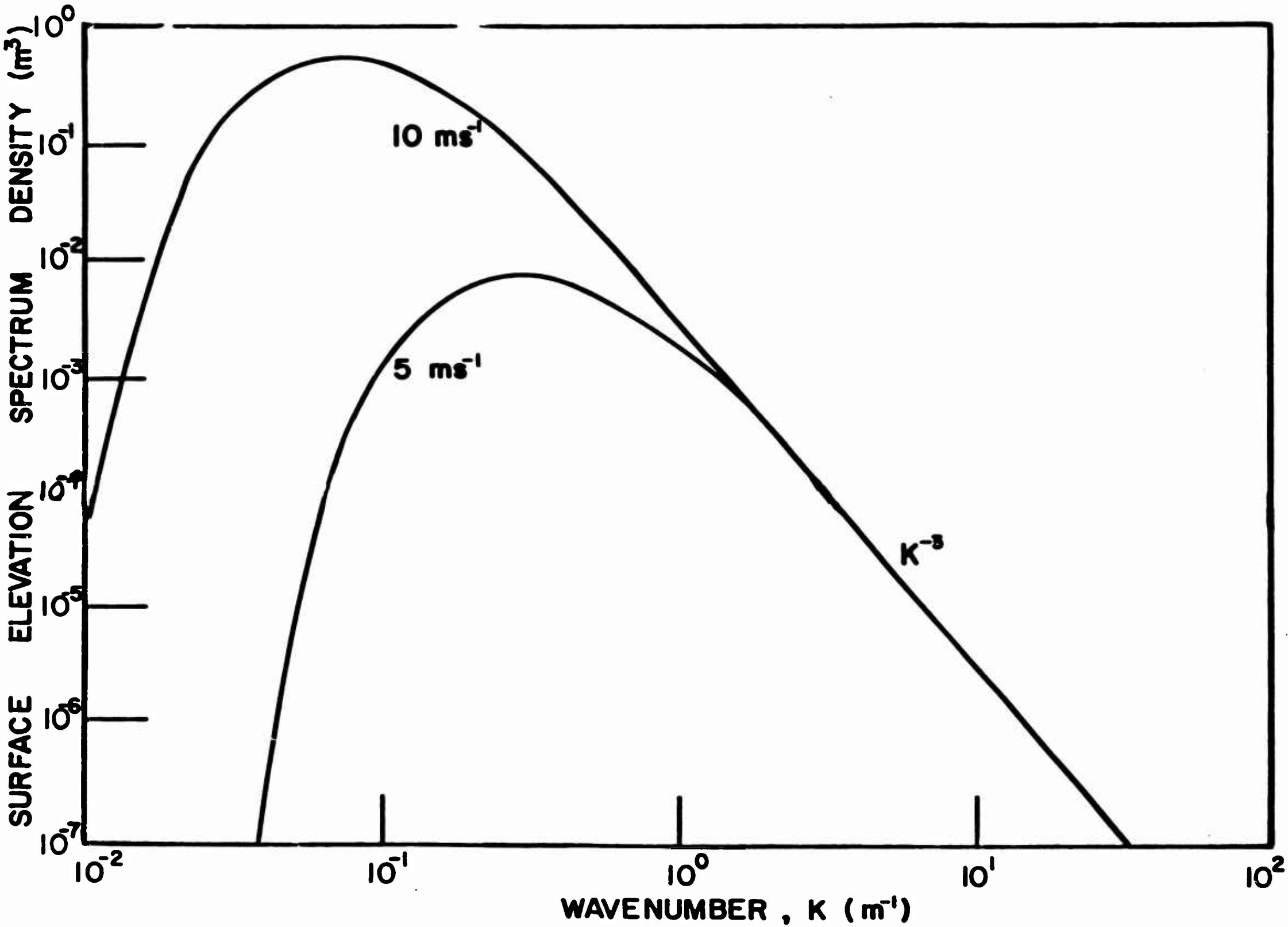

SEA SURFACE ELEVATION WAVENUMBER SPECTRUM FOR WIND SPEEDS OF 5 AND 10 METERS/SEC.

FIGURE 1

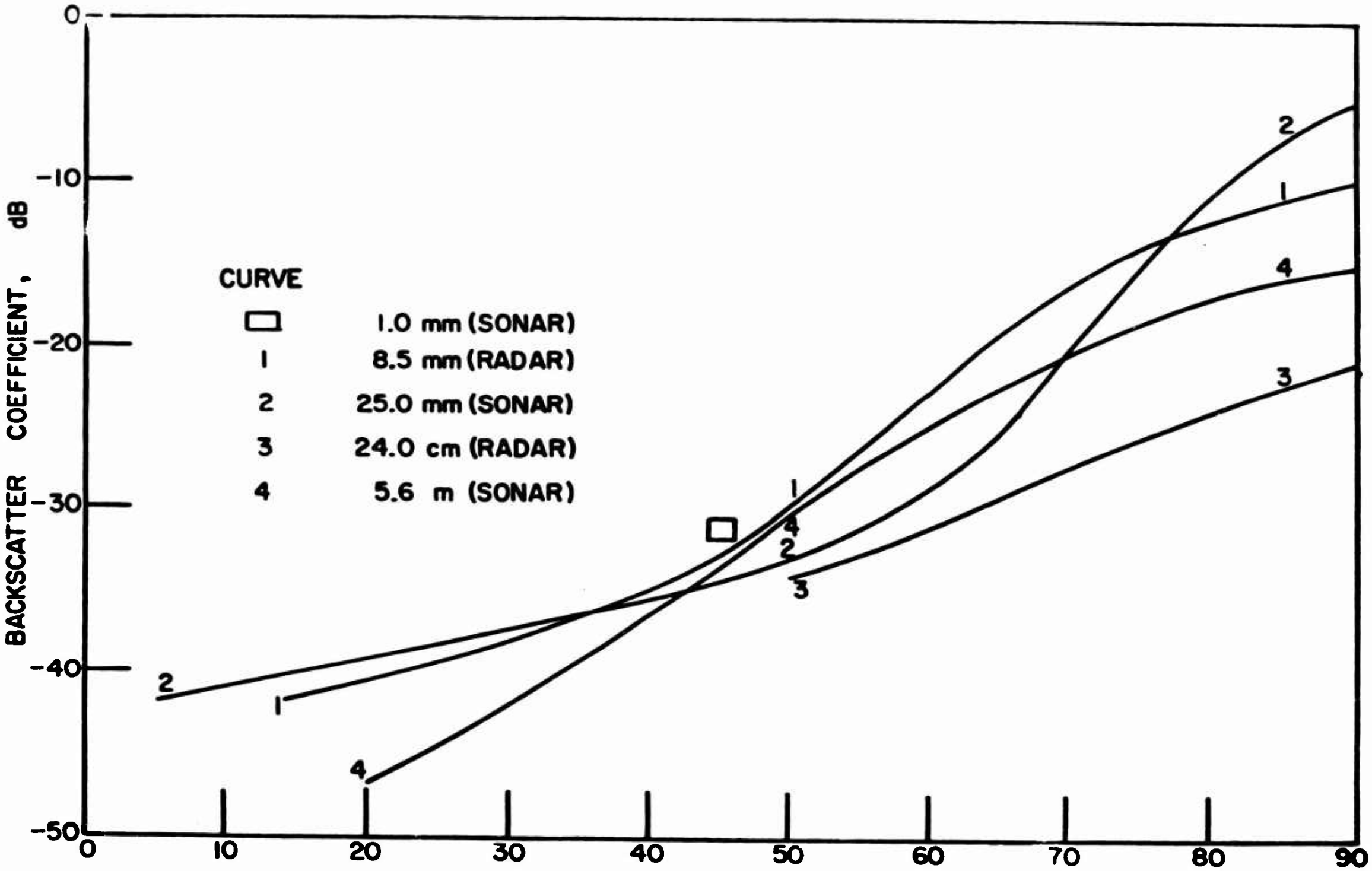

BACKSCATTERING COEFFICIENTS PER UNIT AREA

FIGURE 2

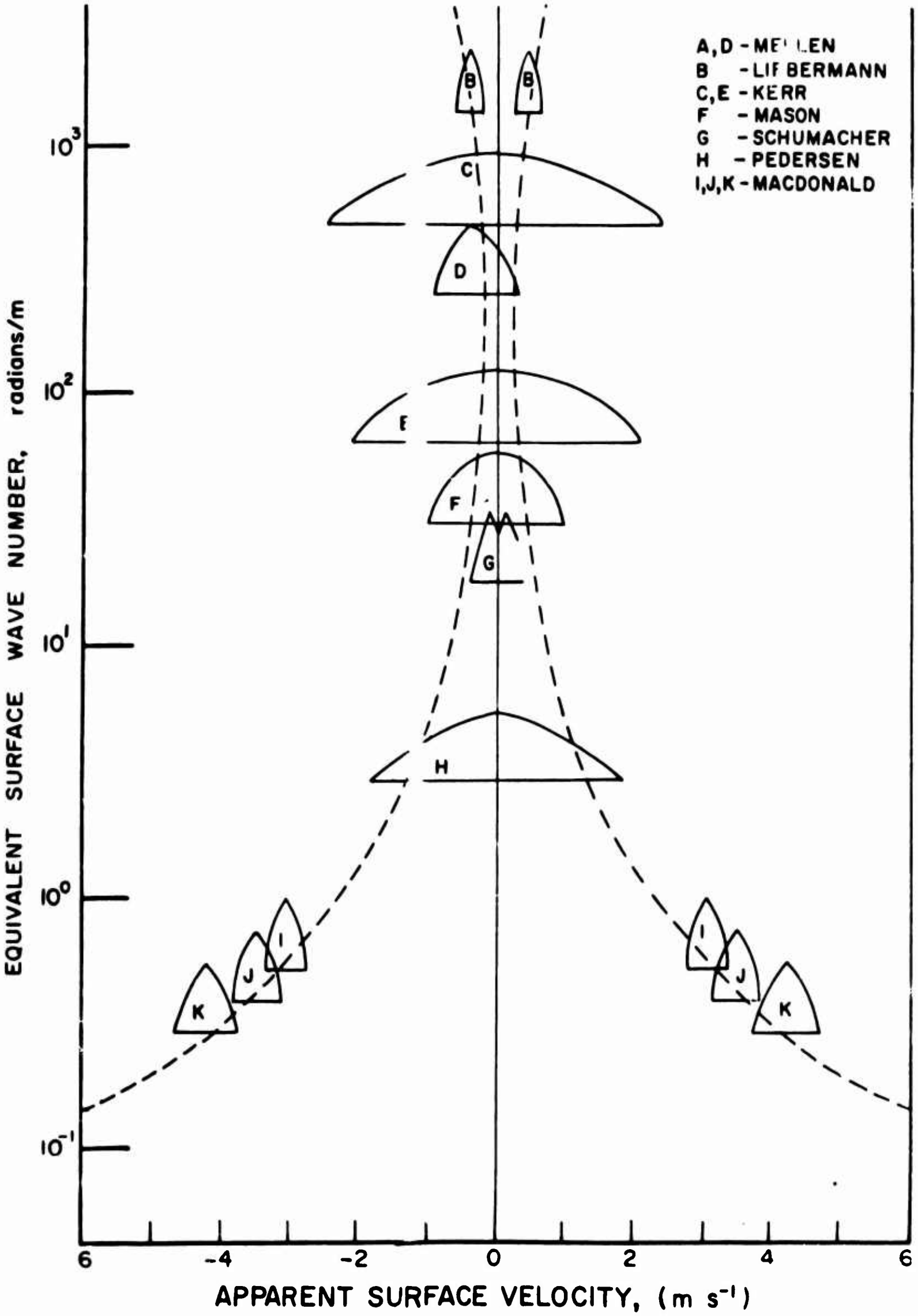

SURFACE WAVE VELOCITY FROM BACKSCATTER DATA

FIGURE 3

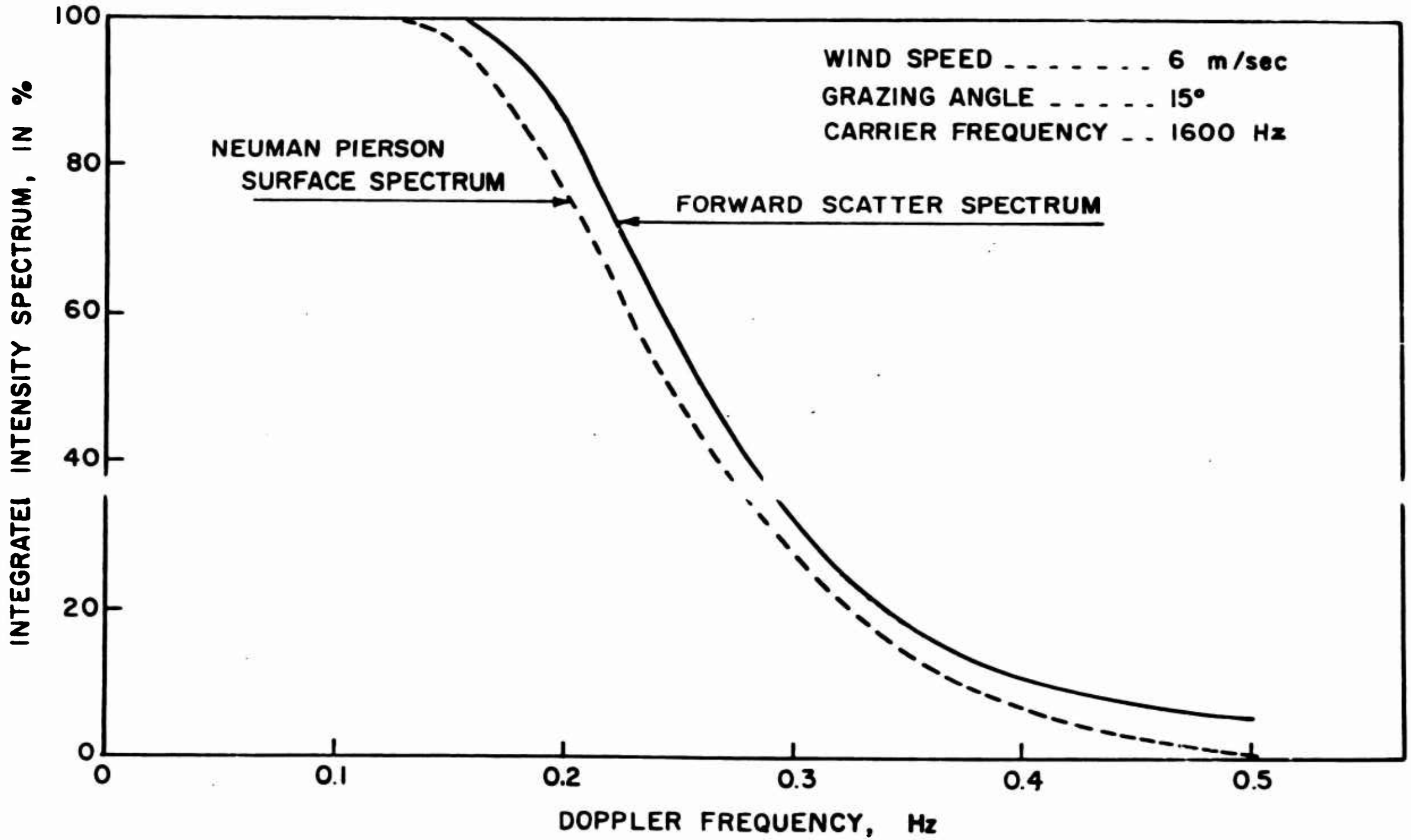

DOPPLER SPECTRUM OF FORWARD SCATTER

FIGURE 4

System Parameters for Ultrasonic Explosive Echo-Ranging

H. W. Marsh *

Abstract

Calculations are presented illustrating the use of high frequencies (up to 40 kHz) for ranging on postulated targets. The high frequencies propagate with acceptable loss because of the finite amplitude of the explosive source. Comparatively high directional discrimination against reverberation and noise can thus be achieved with a receiver of small dimensions.

1 March 1966

* AVCO Marine Electronics Office, New London, Conn.
The research reported here was supported by
The Acoustics Programs, Office of Naval Research
under Contract Nonr 3353 (00).

SYSTEM PARAMETERS FOR ULTRASONIC EXPLOSIVE ECHO-RANGING

INTRODUCTION

The system concept entails a 3.8 lb. Sofar charge, (other sizes can be used), as a source and a directional receiver operating at ultrasonic frequencies, (several tens of kilocylces per second). The novel feature of the system is its high frequency, compared with current practice. Because of the high frequency, directivity is obtainable with a small receiver, providing good resolution for discrimination against reverberation, and ambient noise. Tests[1,2], at sea have proven that the desired frequencies propagate with much lower loss than is true of small amplitude sounds, and indicate that very high signal to interference ratios are achievable for targets at ranges of interest.

No attempt has yet been made to optimize system parameters. Also, full scale tests with an actual target using an adequate receiving system have not been made. However, there is sufficient factual information now available to permit estimation of the performance of postulated systems.

Estimates of performance for the system shown in block diagram, (Figure 1), has been made using the simulation procedures described by Marsh[3].

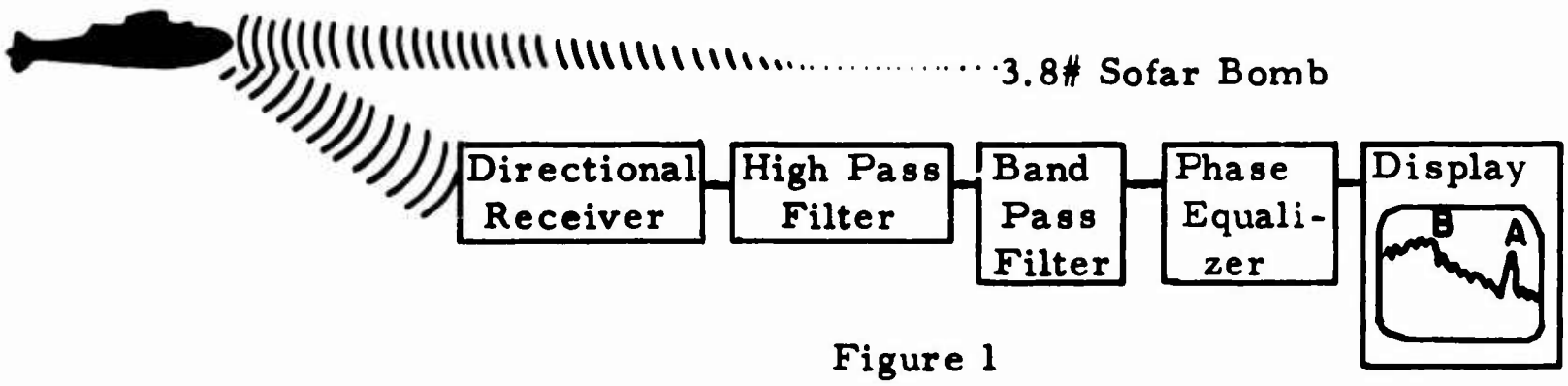

Figure 1

The performance criterion used is peak signal response (A in the Figure), and peak interference (B in the Figure) for a specified observation time.

SIGNAL

The signal input to the receiver is a recording of the direct arrival from a 3.8# Sofar bomb detonated at a range of 6150 meters (the leading edge is shown as I, Figure 9 of Reference 1). The shape of the main arrival from an actual target at a range of 4000 meters is believed to be represented by this form. The rise time is kept small by finite amplitude effects during the 4000 meter path to the target, and then increased normally during the return trip. The rise times t_1 out and t_2 back will tend to add in quadrature (see description following Equation 52 of Reference 1) to produce a net rise time t_3 at the receiver of $(t_1^2 + t_2^2)^{1/2} = t_3$. Peak pressure (broad band) at the target is 100 db//μbar (Figure 10 of Reference 1). Loss in peak amplitude on return trip is estimated to be ,77 dB (Figures 6 and 10 of Reference 2). The effective target strength

is more difficult to estimate. Figures 2-4 show broad band target echos from a beam aspect submarine, at 1500 meters from 1/2# TNT source. The principle echo, which is the main event in Figure 2 and can be identified by arrows in Figures 3 and 4, has an effective target strength of 25dB. The shape of the echo is a close approximation to that of the first positive phase of the direct arrival from the source, which suggests that the target reflection can be taken to be distortionless, but with reduction of amplitude for aspect dependence. Model studies reported by Rubega[4] indicate that the target strength for a quarter aspect fleet hull should be about +7 dB for the short pulses contemplated here. With these assumptions the principle signal arrival at the receiver has an amplitude of 30dB//μbar.

DIRECTIONAL RECEIVER

An 18" diameter spherical lens filled with CCl_4 produces directivity patterns shown in Figure 5. These were measured using a "Homemade" lens fabricated from hand laminated fiberglass. The patterns correspond closely to the theory and measurements of Toulis[5]. The gain shown is relative to 0dB for an omnidirectional hydrophone. This gain, at maximum response can be approximated by a high pass filter with cut-off frequency of 3500 Hz and gain of 25 dB at infinite frequency *.

* Tests recently completed show that the gain is essentially constant at about +25 dB from 20 kHz to at least 100 kHz.

FILTERS

The high pass filter is taken to have a cut-off frequency of 800 Hz, and the band pass to have a center frequency of 40 kHz with Q of 2. 5 (band width = 16 kHz). The high pass is perhaps unnecessary, but is used in the simulation process to make "pink noise", or in other words, to flatten the ambient noise spectrum below 800 Hz. The filter Q appears optimum for the stated center frequency, but the latter is only postulated. Finally, the phase equalizer corrects for phase shift in the pass band, producing some signal enhancement with no effect upon noise.

NOISE SIMULATION

Following Reference 3, an isotropic noise model is used, with a spectrum of the form $(1 + F^2 T^2)^{-1}$, 3 dB down at 800 Hz. This corresponds either to typical ambient noise or to reverberation with a cross section independent of frequency (for the source assumed here).

RESULTS OF SIMULATION

Table I shows the effect of each component of the receiving system upon signal and noise.

TABLE I

SIGNAL		NOISE (Sea State 2)
Input level, peak	+ 30. 0 db/μbar	-
Output from lens	+ 55. 0 db/μbar	-
Output from HP filter	+ 54. 0 db/μbar	+ 1. 0 db/μbar *
Output from BP filter	+ 41. 0 db/μbar	- 20. 0 db/μbar
Output from ∅ equal.	+ 43. 0 db/μbar	- 20. 0 db/μbar

The input peak signal to peak noise after HP filter is +28 dB; the output ratio is + 63 dB. This entails an overall processing gain of 35 dB, of which 25 dB can be attributed to the directional receiver and 10 dB to filtering.

These results can be interpreted in terms of reverberation as the limiting interference. A typical explosive reverberation record is shown in Figure 6. The shot was detonated at a depth of 4000 feet and recorded on a nearby omnidirectional hydrophone. This particular trace was obtained by filtering with a 16-20 kHz bandpass filter, but the trace also typifies results to be expected for the postulated 32-48 kHz filter and the pressure level scale has been adjusted to represent the latter filter. The simulated target return can be seen in proper level and time relationship to the trace. The limiting interference in this case is bottom reverberation. (Note, surface-bottom-surface arrival just before target return).

*rms level is - 9. 7 dB//μbar. Peak levels are for 1. 25 sec processing time.

The water depth was 1800 fathoms - a more favorable geometry could have been achieved with a deeper source and receiver.

RESULTS FOR OTHER RANGES

The situation illustrated in Figure 6 is believed to be a realistic example, for the chosen range of 4000 meters. The signal to reverberation level difference there is + 25 dB; the signal to noise level difference was shown to be + 63 dB. As the range opens the signal to reverberation level difference will diminish it the rate of 3 dB per distance doubled, (boundary reverberation) until volume reverberation becomes dominant, which would be at about 50 km for the situation illustrated. At the 3 dB rate, the signal would still be 15 dB over reverberation at 40 km (for the +7 dB target). Signal to noise level difference will decay more rapidly. The centre frequency should be decreased by about 1/2 for each four fold increase in range, to compensate for increasing absorption. This will produce a loss of 6 dB due to increased noise level and a loss of 6 dB due to decreased direction. Thus optimized, for a four fold increase in range, the signal to noise level difference would decrease by 36 dB from +63 to +27 dB; at 32 km the S/N would be +9 dB. With the reduced frequency, the noise and reverberation levels would be about the same, at the 32 km range.

REFERENCES

1. H. W. Marsh, S. R. Elam and W. L. Konrad,

   Propagation and Reception of Transient Underwater Sounds,
   AVCO Marine Electronics Office, 15 September 1966 (Part I)

2. Ibid, Part II.

3. H. W. Marsh,

   Some Stochastic Structures for Modeling Underwater Sound,
   AVCO Marine Electronics Office, 20 May 1966

4. Robert Rubega,

   Private Communication

5. W. J. Toulis,

   Acoustic Focusing With Spherical Structures,
   J. Acoust. Soc. Am. 35, 286-292 (1963)

FIGURES

1. System Block Diagram
2. Broad Band Echo (50 μsec/cm)
3. Broad Band Echo (500 μsec/cm)
4. Broad Band Echo (400 m sec/cm)
5. Beam Patterns of 18" Spherical lens
6. Typical Explosive Reverberation With Expected Target Echo

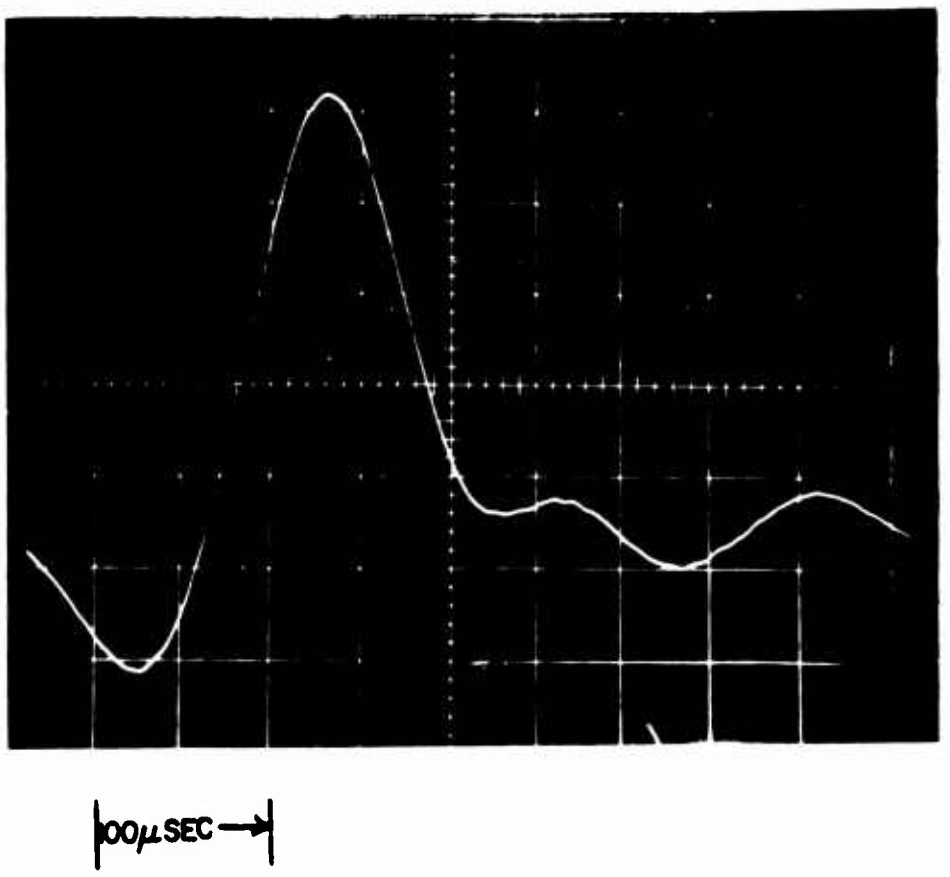

BROAD BAND ECHO (50μSEC/CM)

FIGURE 2

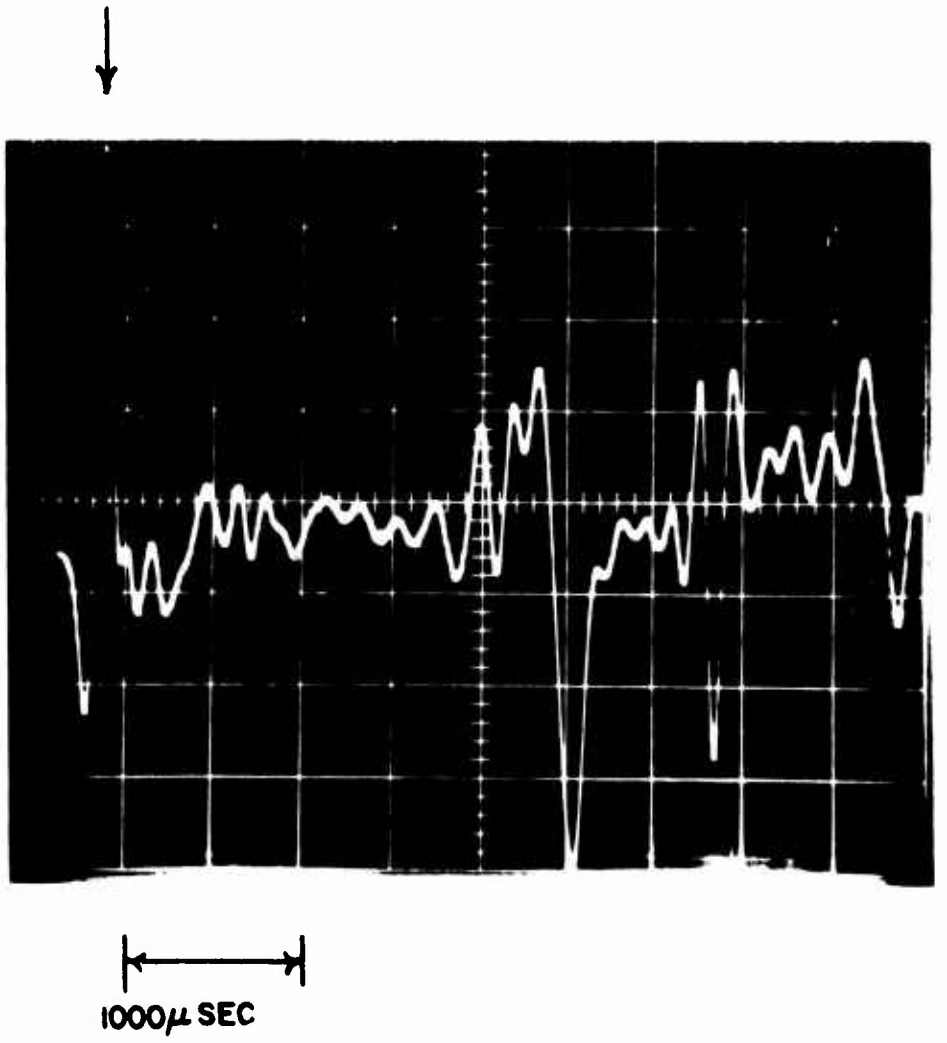

BROAD BAND ECHO (500μSEC/CM)

FIGURE 3

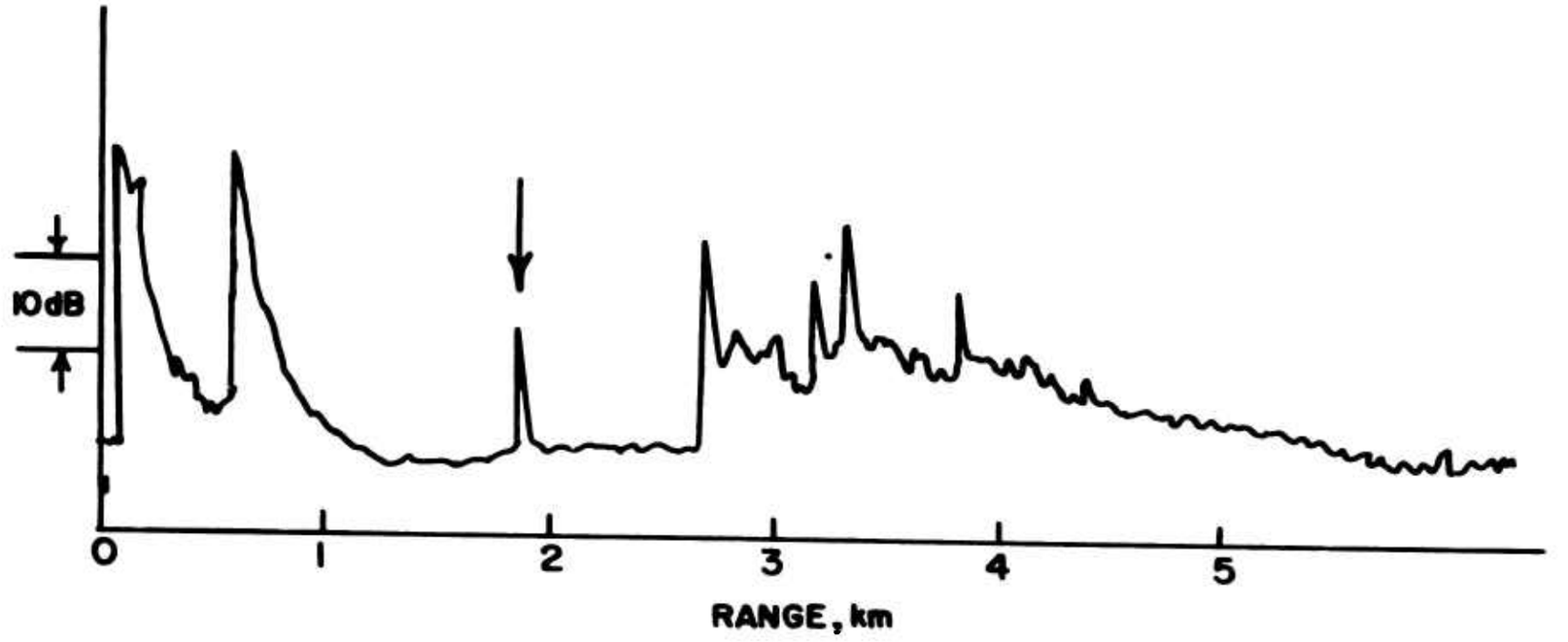

BROAD BAND ECHO (400 m sec/cm)

FIGURE 4

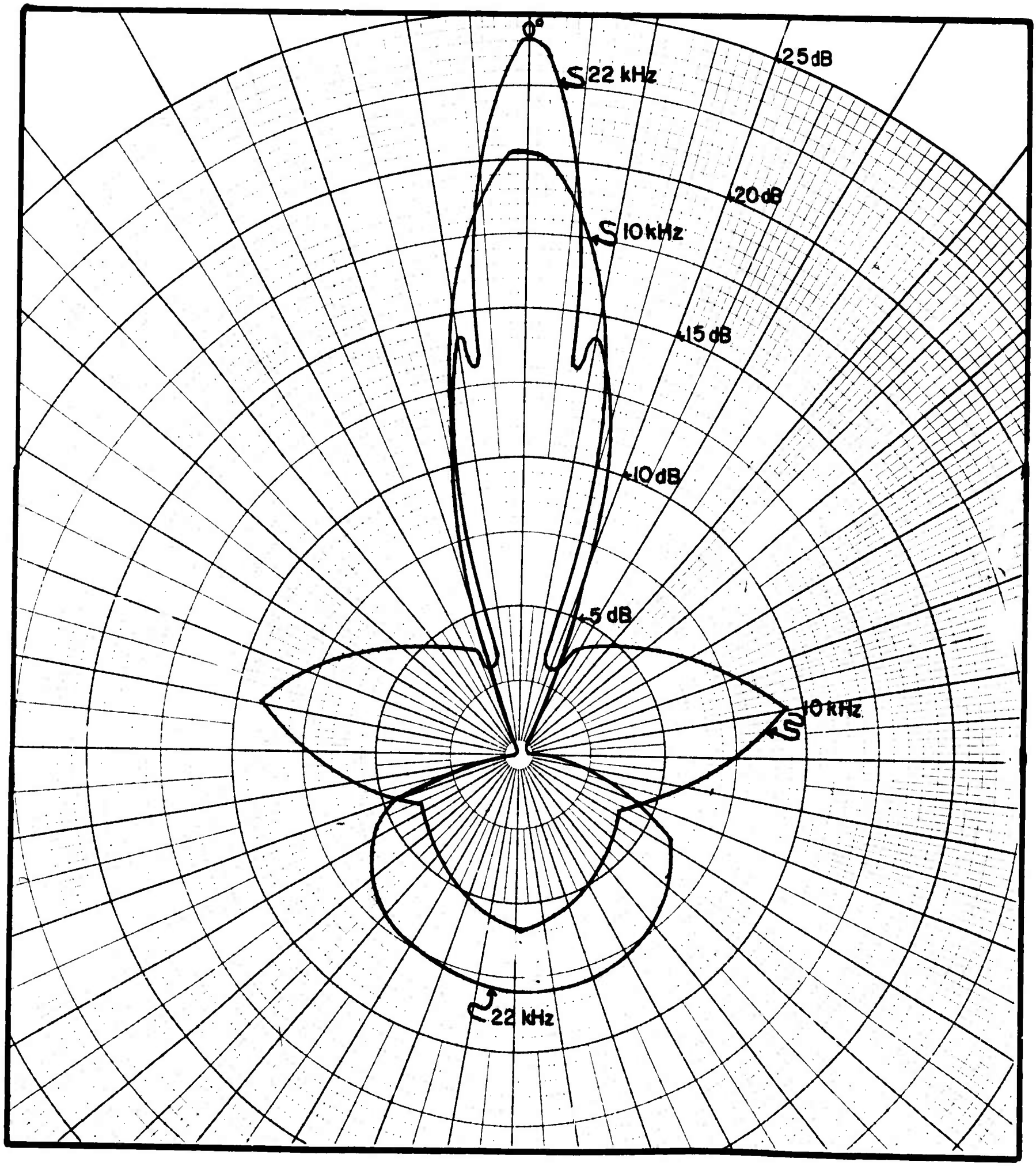

BEAM PATTERN OF 18" SPHERICAL LENS

FIGURE 5

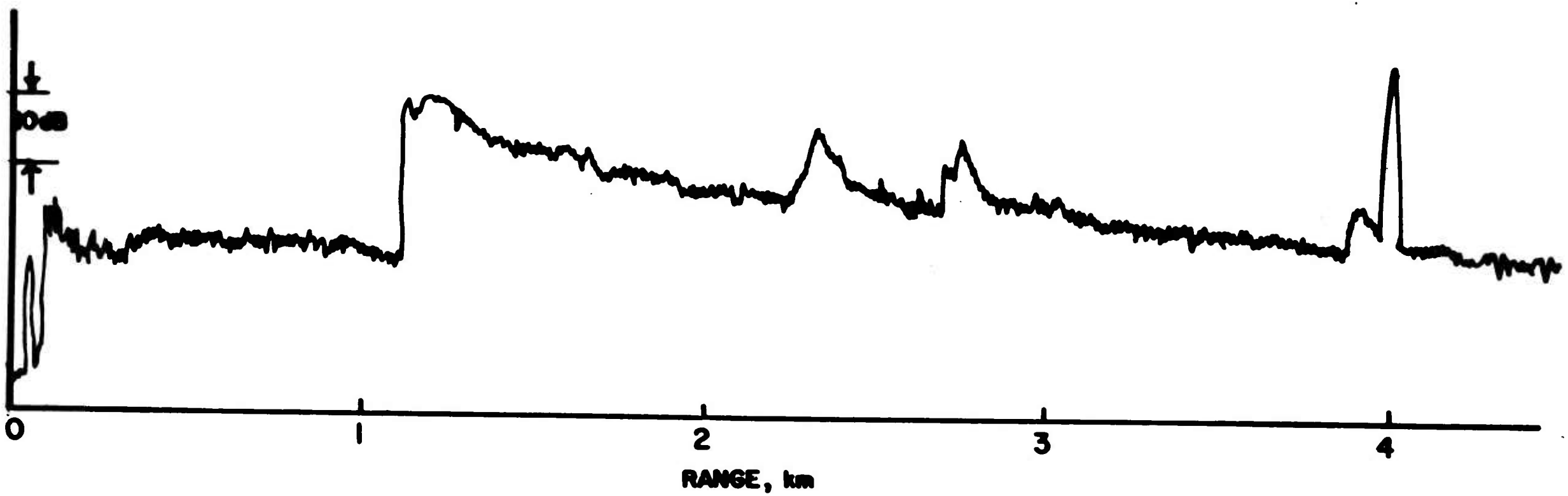

TYPICAL EXPLOSIVE REVERBERATION WITH EXPECTED TARGET ECHO

FIGURE 6

Unclassified
Security Classification

DOCUMENT CONTROL DATA - R&D

(Security classification of title, body of abstract and indexing annotation must be entered when the overall report is classified)

1. ORIGINATING ACTIVITY *(Corporate author)*

AVCO Marine Electronics Office
New London, Conn.

2a. REPORT SECURITY CLASSIFICATION

Unclassified

2b. GROUP

3. REPORT TITLE

Selected Studies of Underwater Sound Phenomena

4. DESCRIPTIVE NOTES *(Type of report and inclusive dates)*

5. AUTHOR(S) *(Last name, first name, initial)*

Marsh, H. W. and Mellen, R. H.

6. REPORT DATE	7a. TOTAL NO. OF PAGES	7b. NO. OF REFS
15 October 1966	36 pages, 15 figures	34

8a. CONTRACT OR GRANT NO.	9a. ORIGINATOR'S REPORT NUMBER(S)
Nonr 3353 (00)	MED-66-1005
b. PROJECT NO.	
c.	9b. OTHER REPORT NO(S) *(Any other numbers that may be assigned this report)*
d.	

10. AVAILABILITY/LIMITATION NOTICES

Distribution is unlimited

11. SUPPLEMENTARY NOTES	12. SPONSORING MILITARY ACTIVITY
	US Navy Office of Naval Research, Washington, D. C.

13. ABSTRACT

This document reports on three separate studies conducted during fiscal 1966 as follows:

Part I, Some Stochastic Structures for Modeling Underwater Sound, discusses simulation of propagation, reverberation and ambient noise with an underlying stochastic description of the sea surface.

Part II, Spectra of The Dynamic Sea Surface proposes a unified model of the equilibrium sea surface, including turbulence and based on observations of several different features of the sea.

Part III, System Parameters for Ultrasonic Explosive Echo-Ranging, illustrates the significance of high frequencies (up to 40 kHz) to permit improved directional discrimination.

DD FORM 1 JAN 64 1473

Unclassified
Security Classification

14. KEY WORDS	LINK A		LINK B		LINK C	
	ROLE	WT	ROLE	WT	ROLE	WT
Underwater Acoustics						
Sonar						
Scattering						
Finite Amplitude Effects						
Ambient Noise						

INSTRUCTIONS

1. **ORIGINATING ACTIVITY:** Enter the name and address of the contractor, subcontractor, grantee, Department of Defense activity or other organization *(corporate author)* issuing the report.

2*a*. **REPORT SECURITY CLASSIFICATION:** Enter the overall security classification of the report. Indicate whether "Restricted Data" is included. Marking is to be in accordance with appropriate security regulations.

2*b*. **GROUP:** Automatic downgrading is specified in DoD Directive 5200.10 and Armed Forces Industrial Manual. Enter the group number. Also, when applicable, show that optional markings have been used for Group 3 and Group 4 as authorized.

3. **REPORT TITLE:** Enter the complete report title in all capital letters. Titles in all cases should be unclassified. If a meaningful title cannot be selected without classification, show title classification in all capitals in parenthesis immediately following the title.

4. **DESCRIPTIVE NOTES:** If appropriate, enter the type of report, e.g., interim, progress, summary, annual, or final. Give the inclusive dates when a specific reporting period is covered.

5. **AUTHOR(S):** Enter the name(s) of author(s) as shown on or in the report. Enter last name, first name, middle initial. If military, show rank and branch of service. The name of the principal author is an absolute minimum requirement.

6. **REPORT DATE:** Enter the date of the report as day, month, year; or month, year. If more than one date appears on the report, use date of publication.

7*a*. **TOTAL NUMBER OF PAGES:** The total page count should follow normal pagination procedures, i.e., enter the number of pages containing information.

7*b*. **NUMBER OF REFERENCES:** Enter the total number of references cited in the report.

8*a*. **CONTRACT OR GRANT NUMBER:** If appropriate, enter the applicable number of the contract or grant under which the report was written.

8*b*, 8*c*, & 8*d*. **PROJECT NUMBER:** Enter the appropriate military department identification, such as project number, subproject number, system numbers, task number, etc.

9*a*. **ORIGINATOR'S REPORT NUMBER(S):** Enter the official report number by which the document will be identified and controlled by the originating activity. This number must be unique to this report.

9*b*. **OTHER REPORT NUMBER(S):** If the report has been assigned any other report numbers *(either by the originator or by the sponsor)*, also enter this number(s).

10. **AVAILABILITY/LIMITATION NOTICES:** Enter any limitations on further dissemination of the report, other than those imposed by security classification, using standard statements such as:

(1) "Qualified requesters may obtain copies of this report from DDC."

(2) "Foreign announcement and dissemination of this report by DDC is not authorized."

(3) "U. S. Government agencies may obtain copies of this report directly from DDC. Other qualified DDC users shall request through

_____."

(4) "U. S. military agencies may obtain copies of this report directly from DDC. Other qualified users shall request through

_____."

(5) "All distribution of this report is controlled. Qualified DDC users shall request through

_____."

If the report has been furnished to the Office of Technical Services, Department of Commerce, for sale to the public, indicate this fact and enter the price, if known.

11. **SUPPLEMENTARY NOTES:** Use for additional explanatory notes.

12. **SPONSORING MILITARY ACTIVITY:** Enter the name of the departmental project office or laboratory sponsoring *(paying for)* the research and development. Include address.

13. **ABSTRACT:** Enter an abstract giving a brief and factual summary of the document indicative of the report, even though it may also appear elsewhere in the body of the technical report. If additional space is required, a continuation sheet shall be attached.

It is highly desirable that the abstract of classified reports be unclassified. Each paragraph of the abstract shall end with an indication of the military security classification of the information in the paragraph, represented as *(TS)*, *(S)*, *(C)*, *or (U)*.

There is no limitation on the length of the abstract. However, the suggested length is from 150 to 225 words.

14. **KEY WORDS:** Key words are technically meaningful terms or short phrases that characterize a report and may be used as index entries for cataloging the report. Key words must be selected so that no security classification is required. Identifiers, such as equipment model designation, trade name, military project code name, geographic location, may be used as key words but will be followed by an indication of technical context. The assignment of links, rules, and weights is optional.